Commun. Comput. Phys.
doi: 10.4208/cicp.311009.191110s

Vol. **9**, No. 5, pp. 1323-1334
May 2011

Comparison of Two Advection-Diffusion Methods for Tephra Transport in Volcanic Eruptions

Kae Tsunematsu[1], Bastien Chopard[2,*], Jean-Luc Falcone[2] and Costanza Bonadonna[1]

[1] *Department of Mineralogy, University of Geneva, 13 Rue des Maraichers, 1205 Geneve, Switzerland.*
[2] *Department of Computer Science, University of Geneva, 7 Route de Drize, 1227 Carouge, Switzerland.*

Received 31 October 2009; Accepted (in revised version) 19 November 2010

Available online 18 February 2011

Abstract. In order to model the dispersal of volcanic particles in the atmosphere and their deposition on the ground, one has to simulate an advection-diffusion-sedimentation process on a large spatial area. Here we compare a Lattice Boltzmann and a Cellular Automata approach. Our results show that for high Peclet regimes, the cellular automata model produce results that are as accurate as the lattice Boltzmann model and is computationally more effective.

AMS subject classifications: 37B15
PACS: 02.60.-x
Key words: Cellular automata, lattice Boltzmann, tephra transport, advection-diffusion, computational efficiency.

1 Introduction

When a volcano erupts explosively, tephra are ejected from the crater within a mixture of gas. Tephra are fragments of magma that travel through the atmosphere and eventually sediment on the ground. Numerical models of tephra transport are important for hazard assessments.

Tephra transport is modeled as an advection-diffusion-sedimentation process. In the air, particles are advected by wind and sediment according to the particle terminal velocity. At the same time, they diffuse as a product of turbulence and small particles ($<125\mu$m) aggregate as a result of particle-particle interaction and atmospheric condition. Field observations show that aggregation significantly affect tephra deposit [3].

*Corresponding author. *Email addresses:* Kae.Tsunematsu@unige.ch (K. Tsunematsu), Bastien.Chopard@unige.ch (B. Chopard), Jean-Luc.Falcone@unige.ch (J. Falcone), Costanza.Bonadonna@unige.ch (C. Bonadonna)

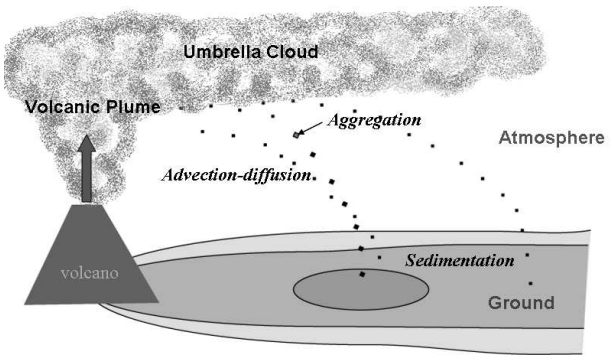

Figure 1: Advection-diffusion-sedimentation process of volcanic tephra transport.

The lattice Boltzmann method (LB) is widely used for advection-diffusion process [4, 7, 8, 11]. However its numerical stability and accuracy depend on calculation parameters. In [11] the stability of the LB advection-diffusion is shown to depend on the Peclet number.

An alternative to the LB approach is the multiparticle Cellular Automata (CA) model designed to describe the transport of passive scalar point particles in a given velocity field $\vec{u}(\vec{r},t)$. This model has been successfully used in [6,9] to describe snow or sand transport and validated on several non-trivial examples of snow accumulation by wind and sand erosion around submarine pipelines. In [12] the application of this CA model to tephra transport is also reported.

In spite of these results and the unconditional stability of the CA scheme, no analytical derivation was ever proposed to describe its behavior in terms of a differential equation, and no studies were conducted to compare its computational efficiency with a LB approach.

In what follows we show that the CA transport model actually obeys an anisotropic advection-diffusion equation. However, this unwanted anisotropy only introduces a small error for system with high Peclet numbers, as is the case in tephra transport. In addition, we show that the unconditional stability of the CA model allows us to choose a coarser discretization than with the LB model. As a result, computations of tephra transport with the CA model can be faster and less memory consuming than with the LB model, yet for a comparable accuracy.

2 The multiparticle cellular automata transport model

The snow and sand transport model proposed in [6,9] is a stochastic multiparticle cellular automata (CA). Each cell contains an arbitrary number of point particles which move to a nearest neighbor cell according to a given advecting field $\vec{u}(\vec{r},t)$. The particles keep their discrete nature all along the process. If needed additional interactions (such as aggregation) between grains that meet on the same lattice site can be added. As far as

passive transport is concerned, the effect of $\vec{u}$ is to give a velocity $\vec{v}_i$ to each of the particle, where $\vec{v}_i$ is a discrete velocity chosen randomly in a set of possible values. The fact that the particles are restricted to move on a lattice introduces a numerical diffusion in the model.

For the sake of illustration we consider here the two-dimensional case. Let us define $\rho(\vec{r},t)$ as the probability to find, at time t, a point particle at spatial location $\vec{r}$ on the lattice. Let us also consider a D2Q9 topology for which the velocity vectors $\vec{v}_i$ ($i=0,\cdots,8$) are defined as

$$\vec{v}_0=(0,0), \qquad \vec{v}_1=(v,0), \qquad \vec{v}_2=(0,v), \tag{2.1a}$$

$$\vec{v}_3=(-v,0), \qquad \vec{v}_4=(0,-v), \qquad \vec{v}_5=(v,v), \tag{2.1b}$$

$$\vec{v}_6=(-v,v), \qquad \vec{v}_7=(-v,-v), \qquad \vec{v}_8=(v,-v), \tag{2.1c}$$

where v is $v=(\Delta x/\Delta t)$, with Δx the lattice spacing and Δt the time step.

We also define $p_i(\vec{r},t)$ as the probability that a particle at position $\vec{r}$ and time t jumps to its nearest neighbor with velocity v_i and reach, at time $t+\Delta t$ the site $\vec{r}+\Delta t\vec{v}_i$.

With these definition the CA transport model can be written as

$$\rho(\vec{r},t+\Delta t)=p_0(\vec{r},t)\rho(\vec{r},t)+\sum_{i\geq 1}p_i(\vec{r}-\Delta t\vec{v}_i,t)\rho(\vec{r}-\Delta t\vec{v}_i,t). \tag{2.2}$$

This equation simply states that the probability to find a particle in $\vec{r}$ at time $t+\Delta t$ is due to the particles at time t that did not move away from r (this happens with probability p_0), plus all the particles reaching r from the neighbors.

Let us assume that $\vec{u}(\vec{r},t)$ is in one of the four quadrant spanned by lattice velocities v_i and v_{i+1}, for $i=1,2,3$ or 4. Let us further assume that due to the action of the advecting field, the particle can have only four possible behaviors. It stays still, moves to $\vec{r}+\vec{v}_i$, $\vec{r}+\vec{v}_{i+1}$, or moves diagonally to $\vec{r}+\vec{v}_i+\vec{v}_{i+1}$. According to the numbering of the velocities $\vec{v}_i+\vec{v}_{i+1}=\vec{v}_{i+4}$, for $i=1,\cdots 4$, if $i+1$ is wrapped onto the values 1 to 4.

In this model, the probability of each of these four movements is determined by the projection of $\vec{u}$ on $\vec{v}_i$ and $\vec{v}_{i+1}$. Therefore the probabilities $p_i(\vec{r},t)$ are built from the advection speed $\vec{u}(\vec{r},t)$ as follows

$$p_i=\frac{\vec{u}\cdot\vec{v}_i}{v^2}\left(1-\frac{\vec{u}\cdot\vec{v}_{i+1}}{v^2}\right), \qquad p_{i+1}=\frac{\vec{u}\cdot\vec{v}_{i+1}}{v^2}\left(1-\frac{\vec{u}\cdot\vec{v}_i}{v^2}\right), \tag{2.3a}$$

$$p_0=\left(1-\frac{\vec{u}\cdot\vec{v}_i}{v^2}\right)\left(1-\frac{\vec{u}\cdot\vec{v}_{i+1}}{v^2}\right), \qquad p_{i+4}=\frac{\vec{u}\cdot\vec{v}_i}{v^2}\frac{\vec{u}\cdot\vec{v}_{i+1}}{v^2}. \tag{2.3b}$$

The other p_j are zero for $j\neq i$, $i+1$, $i+4$. From the above equation it is easy to check that $p_0+p_i+p_{i+1}+p_{i+4}=1$. Since $\vec{u}$ is in the quadrant defined by $\vec{v}_i$ and $\vec{v}_{i+1}$ the scalar product $\vec{u}\cdot\vec{v}_i$ and $\vec{u}\cdot\vec{v}_{i+1}$ are positive and so are the p_i.

3 The anisotropic advection-diffusion equation

We now derive the PDE associated with (2.2), in two dimensions and for a constant $\vec{u}=(u_x,u_y)$. Let us call $\vec{v}_1$ and $\vec{v}_2$ the two lattice velocities that define the quadrant in which $\vec{u}$ lies. According to our notation, the diagonal velocity is labeled $\vec{v}_5=\vec{v}_1+\vec{v}_2$.

The probability $\rho(\vec{r},t)$ is given by (2.2) which, with our notation, reduces to

$$\rho(\vec{r},t+\Delta t)=p_0\rho(\vec{r},t)+p_1\rho(\vec{r}-\vec{v}_1\Delta t,t)+p_2\rho(\vec{r}-\vec{v}_2\Delta t,t)+p_5\rho(\vec{r}-\vec{v}_5\Delta t,t).$$

A Taylor expansion up to order $\mathcal{O}(\Delta t^2)$ gives

$$\partial_t\rho+\frac{\Delta t}{2}\partial_t^2\rho=-\sum_{i=1,2,5}p_iv_{i\alpha}\partial_\alpha\rho+\frac{\Delta t}{2}\sum_{i=1,2,5}p_iv_{i\alpha}v_{i\beta}\partial_\alpha\partial_\beta\rho, \tag{3.1}$$

where indices α and β refer to the spatial components of $\vec{v}_i$ and we used the Einstein summation convention over repeated Greek indices.

The quantity $\sum_{i=1,2,5}p_i\vec{v}_i$ is easily calculated using expressions (2.3b)

$$\begin{aligned}p_1\vec{v}_1+p_2\vec{v}_2+p_5\vec{v}_5&=\frac{\vec{u}\cdot\vec{v}_1}{v^2}\Big(1-\frac{\vec{u}\cdot\vec{v}_2}{v^2}\Big)\vec{v}_1+\frac{\vec{u}\cdot\vec{v}_2}{v^2}\Big(1-\frac{\vec{u}\cdot\vec{v}_1}{v^2}\Big)\vec{v}_2+\frac{\vec{u}\cdot\vec{v}_1}{v^2}\frac{\vec{u}\cdot\vec{v}_2}{v^2}(\vec{v}_1+\vec{v}_2)\\&=\frac{\vec{u}\cdot\vec{v}_1}{v^2}\vec{v}_1+\frac{\vec{u}\cdot\vec{v}_2}{v^2}\vec{v}_2=\vec{u}\end{aligned} \tag{3.2}$$

because $\vec{v}_1$ and $\vec{v}_2$ are orthogonal vectors. Note that this result is valid for any orientation of the coordinate axes.

The other term to be computed in (3.1) is $\sum_{i=1,2,5}p_iv_{i\alpha}v_{i\beta}$. Due to the expression of p_i in terms of $\vec{v}_i$, it produces terms like $\sum_{i=1,2,5}v_{i\alpha}v_{i\beta}v_{i\gamma}$ which actually depends on the choice of the orientation of coordinate system (i.e., the specific value of the components of the $\vec{v}_i$'s). This term is thus not invariant under rotation. We shall compute it for the specific choice of orientation given in (2.1c). Thus $\vec{v}_1$ has only a x-component and $\vec{v}_2$ a y-component. Therefore

$$\begin{aligned}&\frac{\Delta t}{2}\sum_{i=1,2,5}p_iv_{i\alpha}v_{i\beta}\partial_\alpha\partial_\beta\rho\\&=\frac{\Delta tv^2}{2}\Big[\frac{u_x}{v^2}\Big(1-\frac{u_y}{v}\Big)\partial_x^2+\frac{u_y}{v^2}\Big(1-\frac{u_x}{v}\Big)\partial_y^2+\frac{u_y}{v^2}\frac{u_x}{v}\Big(\partial_x^2+2\partial_x\partial_y+\partial_y^2\Big)\Big]\rho\\&=\frac{\Delta tv^2}{2}\Big[\frac{u_x}{v}\partial_x^2+\frac{u_y}{v}\partial_y^2+2\frac{u_xu_y}{v^2}\partial_x\partial_y\Big]\rho\\&=\frac{\Delta tv^2}{2}\partial_x\Big(\frac{u_x}{v}\partial_x+\frac{u_xu_y}{v^2}\partial_y\Big)\rho+\frac{\Delta tv^2}{2}\partial_y\Big(\frac{u_xu_y}{v^2}\partial_x+\frac{u_y}{v}\partial_y\Big)\rho.\end{aligned} \tag{3.3}$$

Then we can write

$$\frac{\Delta t}{2}\sum_{i=1,2,5}p_iv_{i\alpha}v_{i\beta}\partial_\alpha\partial_\beta\rho=\partial_\alpha d_{\alpha\beta}\partial_\beta\rho, \tag{3.4}$$

where the matrix $d_{\alpha\beta}$ is defined as

$$d=\frac{\Delta t v^2}{2}\begin{pmatrix} \frac{u_x}{v} & \frac{u_x u_y}{v^2} \\ \frac{u_x u_y}{v^2} & \frac{u_y}{v} \end{pmatrix}. \tag{3.5}$$

We can now rewrite (3.1) using (3.2), (3.4) and (3.5). It becomes

$$\partial_t\rho+\frac{\Delta t}{2}\partial_t^2\rho=-u_\alpha\partial_\alpha\rho+\partial_\alpha d_{\alpha\beta}\partial_\beta\rho. \tag{3.6}$$

In order to eliminate the second order time derivative in this equation we first differentiate it with respect to time. Neglecting derivatives of 3rd order, the time-derivative of (3.6) gives $\partial_t^2\rho=-u_\alpha\partial_\alpha\partial_t\rho$. And, similarly, $\partial_\alpha\partial_t\rho$ is obtained by a spatial derivative of (3.6), again discarding 3rd order derivatives $\partial_\alpha\partial_t\rho=-\partial_\alpha u_\beta\partial_\beta\rho$, where we have paid attention to change the name of the summation index. Combining the last two equations gives

$$\frac{\Delta t}{2}\partial_t^2\rho=\frac{\Delta t}{2}u_\alpha\partial_\alpha u_\beta\partial_\beta\rho=\frac{1}{2}v^2\Delta t\partial_\alpha\frac{u_\alpha}{v}\frac{u_\beta}{v}\partial_\beta\rho=\partial_\alpha f_{\alpha\beta}\partial_\beta\rho, \tag{3.7}$$

where $f_{\alpha\beta}$ is a lattice contribution to the diffusion matrix whose expression is

$$f=\frac{\Delta t v^2}{2}\begin{pmatrix} \frac{u_x^2}{v^2} & \frac{u_x u_y}{v^2} \\ \frac{u_x u_y}{v^2} & \frac{u_y^2}{v^2} \end{pmatrix}. \tag{3.8}$$

Finally, using (3.7), Eq. (3.6) becomes

$$\partial_t\rho+u_\alpha\partial_\alpha\rho=\partial_\alpha(d_{\alpha\beta}-f_{\alpha\beta})\partial_\beta\rho, \tag{3.9}$$

or, with the diffusion matrix $D_{\alpha\beta}=d_{\alpha\beta}-f_{\alpha\beta}$,

$$D=\frac{\Delta t v^2}{2}\begin{pmatrix} \frac{u_x}{v}-\frac{u_x^2}{v^2} & 0 \\ 0 & \frac{u_y}{v}-\frac{u_y^2}{v^2} \end{pmatrix}, \tag{3.10}$$

the advection-diffusion equation corresponding to the 2D multiparticle CA model is

$$\partial_t\rho+u_\alpha\partial_\alpha\rho=\partial_\alpha D_{\alpha\beta}\partial_\beta\rho. \tag{3.11}$$

We observe that D is anisotropic, even though the lattice diffusion has removed the non-diagonal contributions. This is clearly an unwanted feature of the model as it reflects a non invariance under a rotation of the coordinate axes.

4 Numerical validation

4.1 Anisotropic advection-diffusion

We shall first verify numerically that our CA model obeys Eq. (3.11). The general solution of an anisotropic advection diffusion

$$\partial_t \rho + u_\alpha \partial_\alpha \rho = \partial_\alpha D_{\alpha\beta} \partial_\beta \rho \tag{4.1}$$

is

$$\rho(\vec{r},t) = \sum_{\vec{k}} A_{\vec{k}} e^{-(k_\alpha D_{\alpha\beta} k_\beta)t} e^{i\vec{k}(\vec{r}-\vec{u}t)},$$

where $\vec{k}$ denotes all the possible wave vectors. For a discrete periodic system of size $L_x = N_x \Delta x$ and $L_y = N_y \Delta x$, the acceptable $\vec{k}$s are $\vec{k} = 2\pi(n_x/L_x, n_y/L_y)$, with $n_x \in \{0,1,\cdots,N_x-1\}$ and $n_y \in \{0,1,\cdots,N_y-1\}$.

Here we consider the case of a periodic system of size $L_x = L_y = 1$, in some physical units that we simulate until time $t = 1$, also in some physical units. We choose $N_x = N_y = 20$ and $\Delta t = 0.05$ (in the same units as t). We take $\vec{u} = (0.7, 0.1)v$, where $v = \Delta x/\Delta t$ and $\Delta x = L/N_x$. As an initial condition, we take $\rho(\vec{r},0) = \cos(\vec{k}\cdot\vec{r})$, for $\vec{k} = (2\pi/L)(1,1)$. We observe a very good agreement between simulation and theory, showing that our analytical derivation is correct. Actually it can be checked that the CA obeys Eq. (3.11) up to second order in the lattice spacing Δx. Table 1 gives the error

$$\epsilon \equiv \frac{1}{N_x^2} \sum_{\vec{r}} \left| \rho(\vec{r},t) - \rho_{th}(\vec{r},t) \right|$$

as a function of the discretization. We observe a reduction of the error by a factor 4 as Δx decreases by a factor 2.

Table 1: Value of the error between the analytical expression and the numerical simulation for different discretization level. Here $\Delta x = L/N_x$, $N_x = N_y$, $L = 1$, $T = 1$, $u_x = 0.7v$, $u_y = 0.1v$, and $v = \Delta x/\Delta t$. Note that, when refining the grid we have refined the time accordingly.

N_x	Δt	ϵ
10	0.1	21.3e-4
20	0.05	6.2e-04
40	0.025	1.73e-04
80	0.0125	0.46e-04

4.2 Effective diffusion

Since our model produces an anisotropic diffusion, we may want to know which isotropic diffusion coefficient approximates it best. A natural solution is to define an effective

diffusion coefficient which is the average of D_{xx} and D_{yy}. So we define

$$\bar{D}=\frac{\Delta t v^2}{4}\Big[\frac{u_x}{v}+\frac{u_y}{v}-\frac{u_x^2}{v^2}-\frac{u_y^2}{v^2}\Big]. \tag{4.2}$$

We shall now study the behavior of our model in the case of a symmetrical and localized initial condition given by

$$\rho(\vec{r},0)=a\ \exp\Big[-\frac{(x-L/2)^2+(y-L/2)^2}{2b^2}\Big],$$

where a and b are some parameters.

The time evolution of such an initial condition, subject to an advection-diffusion process, is from [11]

$$\rho(\vec{r},0)=\frac{ab^2}{b^2+2\bar{D}t}\exp\Big[-\frac{(x-L/2-u_x t)^2+(y-L/2-u_y t)^2}{2b^2+4\bar{D}t}\Big]. \tag{4.3}$$

Note that this solution assumes an infinitely large system. With a finite computational domain, t should be chosen small enough so that the boundary conditions do not play a role.

We now consider a numerical experiment in which our CA model shows its undesired anisotropic diffusion due to the fact that $u_x\neq u_y$. In order to estimate the importance of this model artifact, we compare the result of a numerical simulation with the prediction of (4.3).

We choose $L=1$, $N_x=40$, $t=0.4$, $\Delta t=0.025$, $a=1$ and $b=2\Delta x$. Different advecting speeds are considered. When $\vec{u}$ is along the diagonal of the lattice, the diffusion tensor D reduces to a scalar value and the CA model is isotropic. Otherwise, D has two different components and the situation is anisotropic.

To compare the CA model with the theoretical solution of an isotropic advection-diffusion with effective diffusion $\bar{D}$, we consider the error ϵ defined as

$$\epsilon\equiv\frac{\sum_{\vec{r}}|\rho_{th}(\vec{r},t)-\rho(\vec{r},t)|}{\sum_{\vec{r}}\rho_{th}(\vec{r},t)}.$$

As opposed to [11] we no longer normalize the error by N_x^2 because ρ is localized in a small region of the space. With our choice of parameter, the N_x^2 normalization would artificially decrease the error by a factor $64=N_x^2/\sum_{\vec{r}}\rho_{th}(\vec{r},t)=1600/25$.

Table 2 summarizes our results and quantifies the importance of the undesired anisotropy of the model. For high Peclet number, the accuracy of the CA model is then pretty good. The Peclet number is computed as $Pe=uL/\bar{D}=4N_x/(1-(u/v))$.

Note that the error we obtain here are comparable in magnitude with those reported in [11], not even taking into account the difference of normalization. Therefore, in the anisotropic case, the CA model performs only slightly worse than the D2Q9 LB model (and better than the D2Q5).

Table 2: Value of the error between the analytical expression and the numerical simulation for different Peclet number and either an anisotropic or an isotropic situation. Here $L=1$, $\Delta x=L/N_x$, $N_x=N_y$, $\Delta t=0.025$ and $v=\Delta x/\Delta t$.

	Pe	$\vec{u}/v$	t	ϵ
anisotropic	377	(0.1,0.7)	0.4	0.1
isotropic	377	(0.7,0.7)	0.4	0.025
isotropic	11314	(0.99,0.99)	0.2	0.0033
anisotropic	16000	(0.99,0)	0.2	0.0064

5 Stability analysis and calculation efficiency

When running either the CA or the LB simulations, the cell size Δx and time step Δt should be chosen as large as possible in order to reduce the computational work and memory requirement. However, accuracy and stability constraints set a limit to the maximum value we can choose.

To specify the physical parameters of the problem, we choose the example of the Askja volcano 1875 eruption (unit D) [10]. During this eruption, volcanic plume reached a 26km height [2]. The height of the bottom of the umbrella cloud (H_{cb}) where tephra start to fallout, can be estimated to 14.6km with derivation from [1]. Grain size distribution of the tephra on the ground was studied in the field from the vent to 200km far from the vent. Therefore, the calculation domain should be 14.6km$\times$200km. Wind velocity model is suggested by [1]: it varies with height and the maximum wind is 28m/s at the height of tropopause. However, we can use constant wind velocity 25m/s for simplicity. The particle terminal velocity depends on the altitude. It is given in [1], assuming a spherical particle model. The travel time of a particle until sedimentation on the ground (i.e., the duration of the simulation) can be estimated without diffusion. For the smallest particles, it is around 80000 seconds. Grain-size analysis of the ground sediments is done by [10]. In this report, grain size varies from -9ϕ to 4ϕ (ϕ is defined as $\phi=-\log_2 d$, where d is particle diameter in mm). The average grain size is -2.3ϕ. The mean terminal velocity of the mean grain size is around 5m/s. Therefore, advection speed is $\vec{u}=(25,-5)$, i.e., $|\vec{u}|$=27 m/s. Diffusion coefficient of tephra fall range from $\approx 5\times 10^{-5}$ to $\approx 100\text{m}^2/\text{s}$ vertically, and from ≈ 100 to $\approx 10^4\text{m}^2/\text{s}$ horizontally [5]. As an applicable value for both horizontal and vertical directions, we can choose the diffusion coefficient $D=100\text{m}^2/\text{s}$. All the parameters of tephra transport are listed in Table 3.

We have analyzed the stability of LB model by numerical experiments corresponding to the Askja 1875 eruption. The advection speed u and the diffusion coefficient D are given. The parameters that will impact the stability are the lattice spacing Δx and the time step Δt. Alternatively, we can explore the stability region in terms of Δx and the Courant number γ, defined as $\gamma=u\Delta t/\Delta x$. Then Δt can be written as

$$\Delta t=\Delta t(\Delta x,\gamma)=\gamma\frac{\Delta x}{u}. \tag{5.1}$$

Table 3: Parameters of tephra transport (Askja 1875 eruption).

Parameter	**Value**	**unit**
Domain Width	200	km
Domain Height	14.6	km
Duration of simulation	80000	s
Wind Velocity	25	m/s
Mean grain size	-2.3	ϕ
Mean advection speed	27	m/s
Diffusion coefficient	100	m^2/s

The diffusion coefficient D of the LB advection-diffusion model is reported for instance in [4, 8, 11], as a function of the so called relaxation time parameter $\tau > 1/2$. For a given D, τ is a function of Δx and γ

$$\tau = \frac{2D\Delta t}{(\Delta x)^2} + \frac{1}{2} = \frac{2D\gamma}{u\Delta x} + \frac{1}{2}. \tag{5.2}$$

From Eqs. (5.1) and (5.2), we fully specify the LB simulation, for any choice of Δx and γ. Fig. 2 shows the measured stability region in the Δx-γ plane. Note that in our numerical experiment we used a terminal velocity which varies with the height [1], which put extra constraints on the stability of the LB model compare to [11].

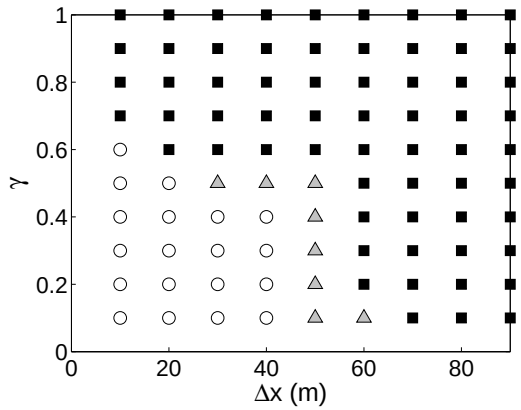

Figure 2: Result of stability analysis, for u and D given. Black squares are unstable points. Gray triangles are stable but the sum of the density has negative value. White circles are stable points. Among these points, we can find the maximum Δx and maximum γ which is $\Delta x = 40$ and $\gamma = 0.4$.

The maximum γ and Δx are chosen within the clearly stable region of Fig. 2. The maximum cell size Δx and time step Δt are then found to be $\Delta x = 40$m, $\Delta t = 0.59$s (LB).

For the CA model, the effective diffusion coefficient is

$$D = \frac{\Delta t v^2}{2}\left(\frac{u}{v}\right)\left(1 - \frac{u}{v}\right). \tag{5.3}$$

By substituting Courant number $\gamma = u/v = u\Delta t/\Delta x$, we can get

$$D = \frac{\Delta x}{2} u(1-\gamma), \quad \text{and thus} \quad \Delta x = \frac{2D}{u(1-\gamma)}. \tag{5.4}$$

The CA simulation is unconditionally stable but it is necessary to have $\gamma < 1$ all over the calculation. Therefore, we chose $\gamma = 0.96$, which then gives $\Delta x = 400$m and $\Delta t = \gamma \Delta x/u = 1.92$s (CA).

We thus observe that the cell size Δx is 10 times larger than that of LB model and the time step Δt is about 3 times longer than in the LB model.

With the above choices of Δx and Δt, we can analyze the computational efficiency of both solvers.

LB efficiency In each site of LB model, we have $Q = 4$ distribution functions with a D2Q4 model (Table 4). Realistic value of particle distribution (e.g., $G = 13$ for Askja volcano) are necessary for a comprehensive story of tephra dispersal and sedimentation. Therefore memory usage of LB model is proportional to $N_{site} \times Q \times G$, where $N_{site} = 1.8 \times 10^6$. Its computational work is proportional to the total number of site updates. The number of iterations is $I = T/\Delta t = 1.36 \times 10^5$, where T is the physical time which is simulated.

$$\text{Memory} \propto N_{site} \times Q \times G = 1.83 \times 10^6 \times 4 \times 13 = 9.51 \times 10^7,$$
$$\text{Computational work} \propto N_{site} \times I \times G = 1.83 \times 10^6 \times 1.36 \times 10^5 \times 13 = 3.23 \times 10^{12}.$$

Table 4: Parameters of calculation.

		LB	**CA**
Δx	Cell Size	40	400
Δt	Time step	0.59	1.92
N_{site}	Number of site	1.83×10^6	1.8×10^4
I	Number of iteration	1.36×10^5	4.17×10^4
P	Number of particle		10^5
Q	Number of velocities	4 (D2Q4)	
G	Number of grain-size class	13	13

CA efficiency In the CA model, the memory scales as $N_{site} \times G$ because, for each class of grain size, we only need to store an integer value corresponding to the number of particles of that size.

For the particle movement, different types of update schemes can be considered [6, 9]. The slowest one requires to move each particle one by one, according to random numbers. In that case, the CPU time grows as $N_{site} + P$, where here $P = 10^5$ is the total number of transported particles over the full system, and $N_{site} = 1.8 \times 10^4$ is the number of site of the CA lattice. For the case of the Askja eruption, the full calculation takes a few hours on a standard laptop (Intel(R) Core(TM)2 Duo CPU at 2.26GH and 1968MB ram).

Table 5: Comparison of calculation efficiency. Here, computational work refers to the total number of site updates.

	LB	**CA**
Memory	9.51×10^{7}	2.34×10^{5}
Computational work	3.23×10^{12}	9.76×10^{9}

In a faster updated scheme, the particles are moved by blocks, assuming a Gaussian distribution for the choice of directions [9]. In this case, the CPU time scales as $N_{site}\times G$. Note that both approaches keep the discrete nature of the particles all along the process and include fluctuations.

But a much faster way is to simulated the real-valued density resulting from the CA dynamics, directly with Eq. (2.2), according to the local values of the p_i's. Then the CPU time is reduced to a few minutes on a laptop. The computational work of this approach goes as the total number of site $N_{site}\times G$ multiplied by the number of iterations $I=4.17\times10^{4}$.

$$\text{Memory} \propto N_{site}\times G = 1.8\times10^{4}\times13 = 2.34\times10^{5},$$
$$\text{Computational work} \propto N_{site}\times G\times I = 1.8\times10^{4}\times13\times4.17\times10^{4} = 9.76\times10^{9}.$$

The result of the comparison is shown in Table 5. We observe that both memory and computational work are two orders of magnitude larger for the LB model. For high Peclet numbers, the intrinsic anisotropy of the CA model is negligible and we can conclude that, for tephra transport, the CA approach is computationally more appropriate than the LB, at least if we use Eq. (2.2) to update the density of transported particles. As to accuracy, our observation (not shown here) is that both the CA and LB model give consistent results which are well within the precision limits of the field observations.

6 Conclusions

We compared two numerical models for advection-diffusion-sedimentation: a multiparticle CA and a LB model. We gave a mathematical description of the CA model and showed that, up to second order in time and space, it simulates an advection process with anisotropic diffusion. However, for high Peclet numbers, the behavior of the model can be well approximated by an effective isotropic diffusion coefficient.

We determined the parameters of the LB model that give the fastest simulation of the transport of tephra in the 1875 eruption of the Askja volcano. Due to numerical stability constraints, the mesh size and time step of the LB method must be much smaller than that for the CA model, which is unconditionally stable. This causes an increase of about two orders of magnitude in the time and space complexity of the LB method as compared to the CA method. In terms of accuracy, both methods are of the same level, in spite of the difference in the space and time discretization.

As discussed in the introduction, particle aggregation significantly affects tephra deposit. Therefore, we are planning to describe particle aggregation with our CA model which provides a suitable framework for particle-particle interaction process.

Acknowledgments

This work is supported by the Swiss National Science Foundation and the European Commission (COAST project EUFP6- IST-FET Contract 033664).

References

[1] C. Bonadonna, and J. C. Phillips, Sedimentation from strong volcanic plumes, J. Geophys. Res., 108(B7) (2003), 2340–2368.
[2] S. Carey, and R. S. J. Sparks, Quantitative models of the fallout and dispersal of tephra from volcanic eruption columns, Bull. Volcanol., 48 (1986), 109–125.
[3] S. N. Carey, and H. Sigurdson, Influence of particle aggregation on deposition of distal tephra from the May 18, 1980, eruption of mount st helens volcano, J. Geophys. Res., 87(B8) (1982), 7061–7072.
[4] B. Chopard, J. L. Falcone, and J. Latt, The lattice Boltzmann advection-diffusion model revisited, Europhys. J., 171 (2009), 245–249.
[5] A. Costa, G. Macedonio, and A. Folch, A three-dimensional eulerian model for transport and deposition of volcanic ashes, Earth. Planet. Sc. Lett., 241 (2006), 634–647.
[6] A. Dupuis, and B. Chopard, Lattice gas modeling of scour formation under submarine pipelines, J. Comput. Phys., 178 (2002), 161–174.
[7] I. Ginzburg, Equilibrium-type and link-type lattice Boltzmann models for generic advection and anisotropic-dispersion equation, Adv. Water. Res. Pages., 28(11) (2005), 1171–1195.
[8] Z. L Guo, B. C. Shi, and N. C. Wang, Fully lagrangian and lattice Boltzmann methods for the advection-diffusion equation, J. Sci. Comput., 14(3) (1999), 291–300.
[9] A. Masselot, and B. Chopard, A lattice Boltzmann model for particle transport and deposition, Europhys. Lett., 42 (1998), 259–264.
[10] R. S. J. Sparks, L. Wilson, and H. Sigurdsson, The pyroclastic deposites of the 1875 eruption of askja, Iceland, Philos. Trans. R. Soc. London., 299 (1981), 241–273.
[11] S. Suga, Numerical schemes obtained from lattice Boltzmann equations for advection diffusion equations, Int. J. Mod. Phys. C., 17(11) (2006), 1563–1577.
[12] K. Tsunematsu, J. L. Falcone, C. Bonadonna, and B. Chopard, Applying a cellular automata method for the study of transport and deposition of volcanic particles, ACRI 2008 proceedings, LNCS 5191, pages 393–400, 2008.